

## ALONG-TRACK INTERFEROMETRY (ATI) OBSERVATIONS OF CURRENTS AND FRONTS IN THE TAY ESTUARY, SCOTLAND

*J. Trevor Macklin<sup>1</sup>, Graham Ferrier<sup>2</sup>, Simon Neill<sup>3</sup>, Graham Copeland<sup>4</sup> and Andrew Folkard<sup>5</sup>*

1. Communications and Signal Processing Department, BAE SYSTEMS Advanced Technology Centre, Great Baddow, Chelmsford, Essex CM 2 8HN, England; [trevor.macklin\(at\)baesystems.com](mailto:trevor.macklin@baesystems.com)
2. Department of Geography, University of Hull, Hull, HU6 7RX, England; [g.ferrier\(at\)hull.ac.uk](mailto:g.ferrier@hull.ac.uk)
3. Centre for Applied Oceanography, University of Wales Bangor, Menai Bridge, Anglesey, LL59 5AB, Wales; [s.p.neill\(at\)bangor.ac.uk](mailto:s.p.neill@bangor.ac.uk)
4. Department of Civil Engineering, University of Strathclyde, 107 Rottenrow, Glasgow, G4 0NG, Scotland; [g.m.copeland\(at\)strath.ac.uk](mailto:g.m.copeland@strath.ac.uk)
5. Department of Geography, Lancaster University, LA1 4YB, England; [a.folkard\(at\)lancaster.ac.uk](mailto:a.folkard@lancaster.ac.uk)

### ABSTRACT

Existing boat-based methods are unable to measure current fields with sufficient spatial coverage for accurate modelling of hydrodynamic processes in estuaries. This means that present models are limited in their ability to predict the dispersion of pollution and sediment. Remotely-sensed data offer more extensive spatial coverage. However, previous studies based on conventional optical, thermal and radar imaging sensors have failed to obtain sufficient temporal coverage in order to map the details of the current field. The new technique of along-track interferometry (ATI) is attractive because it can estimate the instantaneous surface flow from a single pass over a whole estuary. Here we present some observations over the Tay Estuary, Scotland, which illustrate the benefits of this technique. The results demonstrate the potential for enhancing existing hydrodynamic models of this region.

**Keywords:** along-track interferometry (ATI), synthetic-aperture radar (SAR), estuarine fronts, estuarine currents.

### INTRODUCTION

Estuaries are extremely dynamic environments where large and frequent changes can occur in the bathymetry and in the locations of channels. Because estuaries are major centres of population and industry, there is an on-going requirement to monitor and predict changes in the current fields. The tidal range, surface wind speed, atmospheric pressure, fresh water inflow and most importantly the stage of the tidal cycle affect the flow vectors.

At present, most agencies responsible for water quality in estuaries employ two-dimensional, depth-averaged numerical models. These models have severe limitations in simulating dispersion of pollution and suspended sediments, particularly in large estuaries. The limitations occur because various complex but important hydrodynamic features are neglected, and because the available measurements to drive the models are only sparsely sampled. Complex interactions of vertical and lateral density gradients with the bathymetry cause regions of intensified horizontal gradients, termed 'fronts', to occur at the interfaces between water bodies of differing salinity in the Tay (1,2). The development of more accurate models requires significantly more quantitative data on the flow fields associated with these fronts, including measurements that show how the fronts form and evolve during the tidal cycle.

Here, we examine the potential of remote-sensing observations to provide relevant information, by using the technique of along-track interferometry (ATI) from synthetic-aperture radar to map the current field. We discuss the results obtained from an experiment over the Tay Estuary, Scotland, on 5<sup>th</sup> June 2000, during the British National Space Centre (BNSC)'s SAR and Hyperspectral Campaign (SHAC).

## STUDY AREA

The Tay Estuary covers an area of 122 km<sup>2</sup> and has a maximum depth of 30 m at the Tayport Narrows (Figure 1). Tides are strongly semi-diurnal, with two high and low waters occurring every 24 h 48 min. The tidal range is 5.8 m (spring) to 4.0 m (neap). The flow fields in the Tay are complicated by the constriction of the estuary at the Tayport narrows and by the complex bathymetry (Figure 1, bottom). Maximum estuarine flow occurs at mid-flood tide, approximately 2.5 hours before high water, on a spring tide. The horizontal velocity gradient, however, varies markedly at different localities in the Estuary and at different tidal stages, with the most complex and rapidly changing flow fields occurring at the Tayport narrows around 0.5 hours before high water.

Fronts occur in a variety of forms in this area. The most significant are tidal intrusion fronts which occur when the denser, intruding sea water (confined laterally by the sides of the estuary) plunges beneath the ambient, estuarine water to form a characteristic V shape (3). Figure 2 shows the type of structure which occurs, and Figures 3 and 4 show examples where such features have been imaged over the Tay, from airborne thermal and visible imagery, respectively.

## OBSERVATIONAL DATA

A range of observational data from boats, airborne remote-sensing data and results from hydrodynamic models has been obtained in studies of the Tay Estuary over many years (Tables 1 and 2). These provide a general understanding of the behaviour of the estuary, which may be combined with both the data obtained and the modelling undertaken around the time of this SHAC experiment.

*Table 1: Summary of boat observations of Tay estuary*

Observation Types	Instrument	Acquisition Date(s)	Properties	Physical Data Acquired
Boat - Acoustic Doppler Current Profiler (ADCP)	RDI - 300 MHz	1998 - 2001	Vertical transects (1-10 m cell size). Blanking Distance (BD) = 2.5 m	Vertical current velocity profiles
Boat - ADCP	Sontek - 1500 MHz	2002	Vertical or horizontal transects (0.1 to 5 m cell size). BD = 0.5 m	Vertical or horizontal current velocity profiles
Boat - surface velocity meter	N/A	1970 - 1996 & 5/6/2000	Continuous surface single point measurement	Surface velocity
Drift buoys	N/A	1970 - 1996	Discrete measurements over a tidal cycle	Surface velocity
Boat - conductivity temperature profiles (CTP)	N/A	1970 - 2003	Continuous single point measurements between surface and 10 m depth	Surface & vertical temperature and salinity profiles

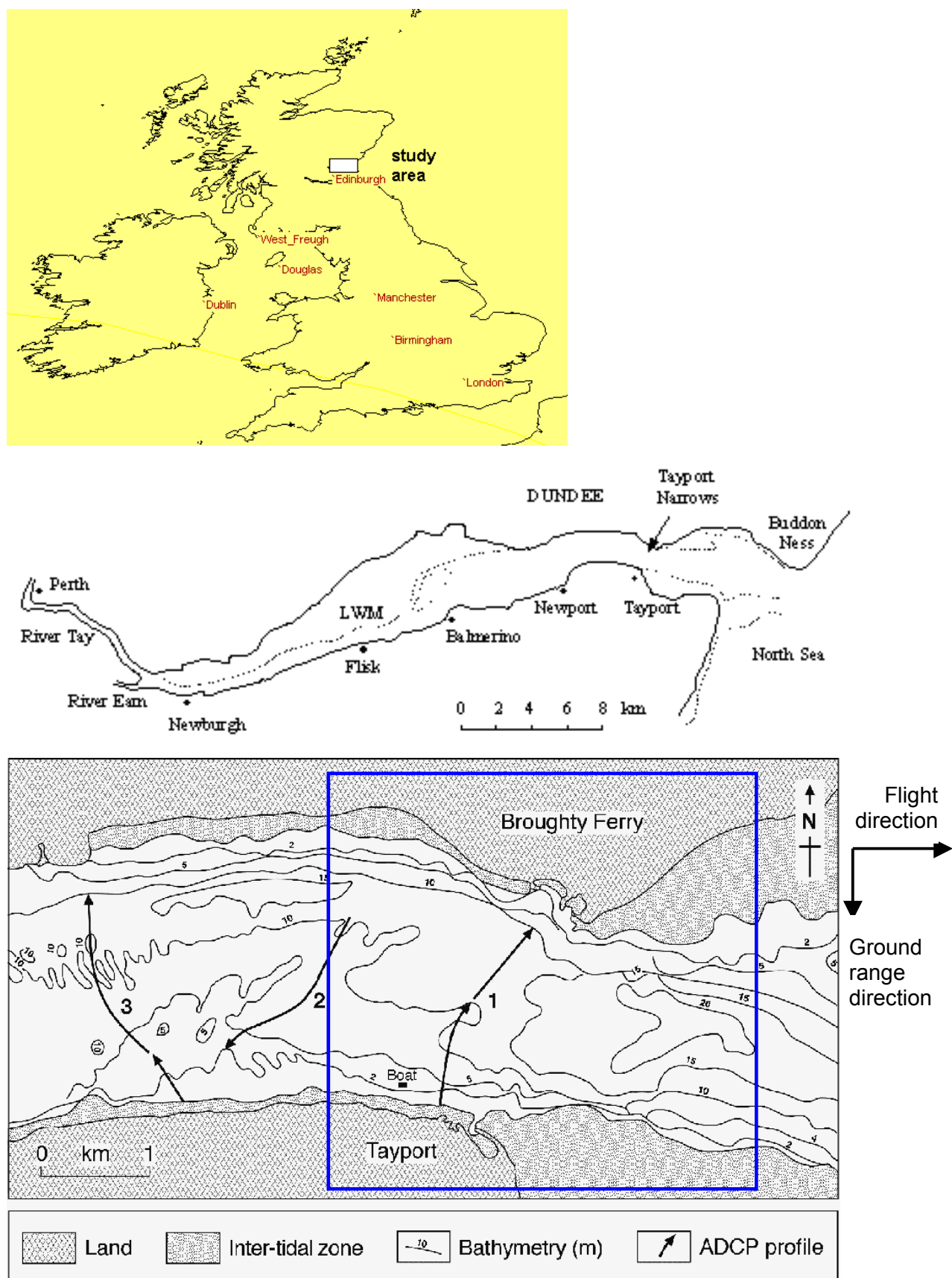


Figure 1: Location of the study area (top) and local bathymetry (bottom). The lines 1, 2 and 3 mark three current-meter transects. The blue box marks the area of the ATI images shown in Figures 5 and 6. The radar flies from east to west and it looks towards the south.

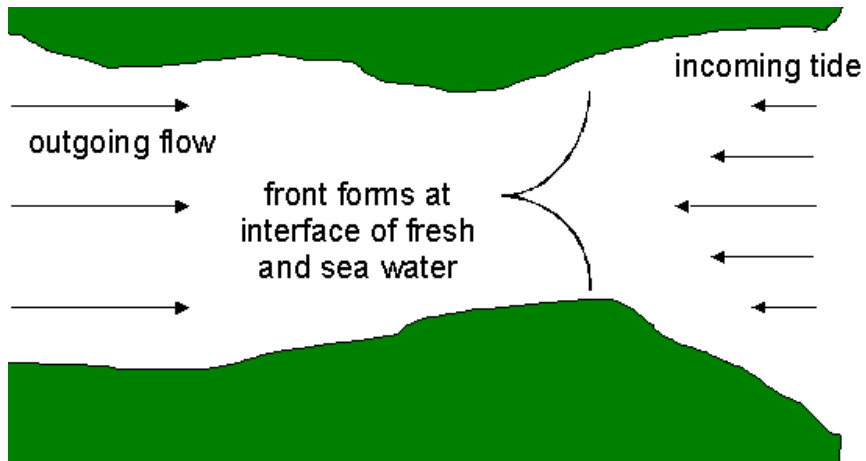


Figure 2: Schematic illustration of predicted surface flow structure around a Tidal Intrusion Front in the Tay Estuary.

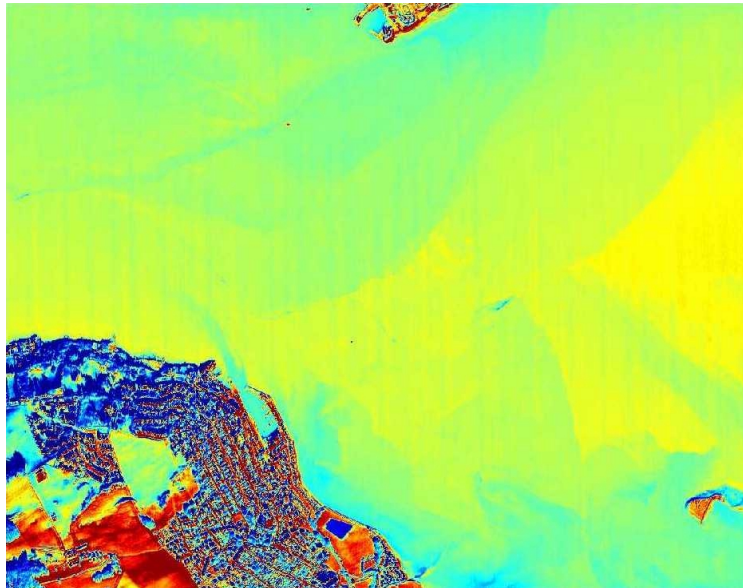


Figure 3: Thermal Infrared image (ATM) of Tayport Narrows area 10 minutes before high water (facing northwards), on 27<sup>th</sup> July 1989, tide height 5.2 m.



Figure 4: Visible image (ATM) of Tayport Narrows area, 10 minutes after high water, on 4<sup>th</sup> September 1991, tide height 4.8 m.

Table 2: Summary of previous airborne remote sensing of Tay estuary

Sensor Type	Instrument Details	Acquisition Date(s)	Types of Observations
Airborne Thematic Mapper (ATM)	11 bands 0.4 to 13.0 micron	1984, 1986, 1988, 1989, 1991, 1994, 1997, 1999, 2000	Visible: water quality, Suspended Sediment Concentration (SSC) NIR: surface features (foam lines) Thermal: Sea surface temperature
Compact Airborne Spectrographic Imager (CASI)	16 to 244 bands 0.4 to 1.1 micron (programmable)	1997, 1999, 2000	Visible: water quality, SSC NIR: surface features (foam lines)

## ALONG-TRACK INTERFEROMETRY OBSERVATIONS

Along-track interferometry (ATI) from synthetic-aperture radar (SAR) is a promising new technique for measuring and mapping the spatial structure of ocean surface velocities. The fundamental principle is that the interferometric combination of two complex SAR images of the same scene, acquired with a short time lag, is sensitive to the component of velocity along the line-of-sight associated with each pixel in the scene. Initial studies (e.g. 4) suggested that the ATI phase would provide a direct measurement of the ocean current. Although more recent studies indicate a more complicated relationship to all the factors which contribute to motion on the sea surface (e.g. 5), the technique still has promise in providing maps of the velocity structure from a single pass.

### Experiment Background and Instrumentation

During SHAC, the DLR polarimetric airborne SAR (ESAR) (6,7), obtained three data-takes over the middle and outer Tay estuary during the mid-flood tidal phase. Two passes of C-band data in conventional SAR image mode, and one pass of X-band data in ATI mode, were acquired. The properties of the radar data are summarised in Table 3. The data are in vertical polarisation and the aircraft altitude was 3.07 km. The ATI data were acquired with an along-track baseline of 0.871 m, which corresponds to a time lag of 9.83 ms between the two components of the interferogram, for the transmit/receive configuration here. (This is the double baseline mode described by (7), where both antennas transmit and receive in a 'ping-pong' mode.)

Note that the time lag needs to be less than about 10 ms at X band in order for the interferogram to be sufficiently coherent to image ocean features, according to (8). Longer time lags may be tolerated at low wind speed. The wind velocity here is low; the measurement at a nearby meteorological station around the time of the ATI data-take was 2.6 m/s, bearing 70°, at 1600 GMT. Hence the time lag is sufficiently short for the imaging of ocean features here.

Table 3: Properties of airborne SAR data obtained over the Tay Estuary in June 2000.

Pass type	Conventional SAR	Conventional SAR	ATI
Time (GMT, 5 <sup>th</sup> June 2000)	15:21 - 15:24	15:59 - 16:01	16:16 - 16:18
Radar frequency	5.3 GHz (C band)	5.3 GHz (C band)	9.6 GHz (X band)
Flight direction (bearing)	-91.2°	89.3°	89.4°
Incidence angle	25° - 58°	25° - 58°	30° - 58°
Swath width (on ground)	3.53 km	3.53 km	3.21 km
Ground speed	86.5 m/s	88.7 m/s	88.6 m/s
Pixel spacing *	1.5 m x 0.35 m	1.5 m x 0.35 m	1.5 m x 0.35 m
Spatial resolution *	2 m x 2 m	2 m x 2 m	2 m x 0.72 m

\* range x azimuth

### Along-Track Interferometry Results

The ESAR data were acquired over a flight path optimising coverage of the Tay estuary along a bearing almost due east ( $89.4^\circ$ ), at 16.18 GMT on 5<sup>th</sup> June 2000, (32 minutes before high water) on a very high tide (5.4m). Figures 5 and 6 show the results from the ESAR observations. An area of the Tay Estuary about 3 km (ground range: vertical) x 2 km (along-track: horizontal) is shown. North is at the top, and the flight direction was west to east. The area shown is just to the east of Dundee, and includes Tayport and Broughty Ferry on the south (bottom) and north (top) shorelines respectively (see Figure 1).

The conventional SAR image (Figure 5, top left) shows a bright linear feature running approximately down the middle of the estuary. Some other linear features branch off from this. The image of the ATI phase (Figure 5, top right) shows that these features generally correspond to abrupt changes in velocity.

The ATI phase  $\phi$  is proportional to the component of velocity along the line of sight of the radar. At the surface, the current is confined to the horizontal plane. The ground range direction is defined as the projection of the line of sight on to the horizontal plane. Hence the component of the current along the line of sight is proportional to  $v_{rs} \sin \theta$ , where  $v_{rs}$  is the component of the surface current in the ground range direction and  $\theta$  is the incidence angle. Thus  $v_{rs}$  is obtained from the following expression which is derived by (4) and (5):

$$v_{rs} = \frac{\lambda_r \phi}{720 \tau \sin \theta} \quad (1)$$

Here, the ATI phase  $\phi$  is expressed in degrees,  $\lambda_r$  is the radar wavelength,  $\tau$  is the time delay between the two components of the interferogram. This expression assumes that the dominant signal comes from short surface waves obeying the Bragg-resonant condition. We would expect this to be a valid approximation for the low wind speeds encountered here (2.6 m/s as noted above). A positive  $v_{rs}$  corresponds to motion away from the radar (towards south here).

Figure 5 (bottom) shows plots of  $v_{rs}$  along two lines which lie on either side of the ADCP transect 1 (shown in Figure 1, bottom). The south end of the green line includes the land at Tayport Harbour at pixels 0 - 160, while the north end of both lines includes the land at Broughty Ferry at pixels 500 - 620 (turquoise) and pixels 560 - 620 (green). We see phase changes over these areas of land because the elevation increases from sea level to about 50 m in these areas. (Much of the land near the coast at Broughty Ferry is low lying and appears dark in Figure 5, middle, especially towards the top right.) The change in phase here is therefore correlated with the topography. It arises because there is a component of the interferometer baseline in the across-track direction associated with yaw of the aircraft platform. Note that the SAR processing includes compensation to correct for fluctuations in motion during the acquisition of the scene. However, the across-track baseline arising from a steady yaw is not compensated.

The across-track baseline also produces a phase gradient across the swath. This occurs because the difference in paths between an imaged point on the ground and each of the two antennas varies with distance for an across-track baseline. This effect produces a difference in the apparent velocities of about 0.5 m/s at the north and south shorelines in Figure 5. We have not attempted to correct this phase gradient in Figure 5 and hence there is a calibration offset in the estimated velocities.

Nevertheless, the striking feature of Figure 5 (top right and bottom) is that there are significant changes in velocity,  $\sim 1$  m/s, over about 20 m either side of the bright linear features in the estuary. (Note, for example, the sharp transitions near pixel 370 in Figure 5, bottom.)

The inferred map of  $v_{rs}$  is shown in Figure 6 (bottom left). This image shows very similar structure to Figure 5 (top right); in fact the two images are related via equation (1). Thus the low-lying land around Broughty Ferry appears as the light blue area towards the top right in Figure 6 (bottom left).

Figure 6 also shows the ATI amplitude (top left) and coherence (top right) on grey scales. The coherence, which expresses the degree of correlation between the signals received at the two ATI antennas, is about 0.6 over the water surface. Lower values tend to occur where the bright linear features occur in the image. The amplitude, phase and coherence together represent the full information content of the ATI data. These are combined as a colour composite in Figure 6 (bottom right).

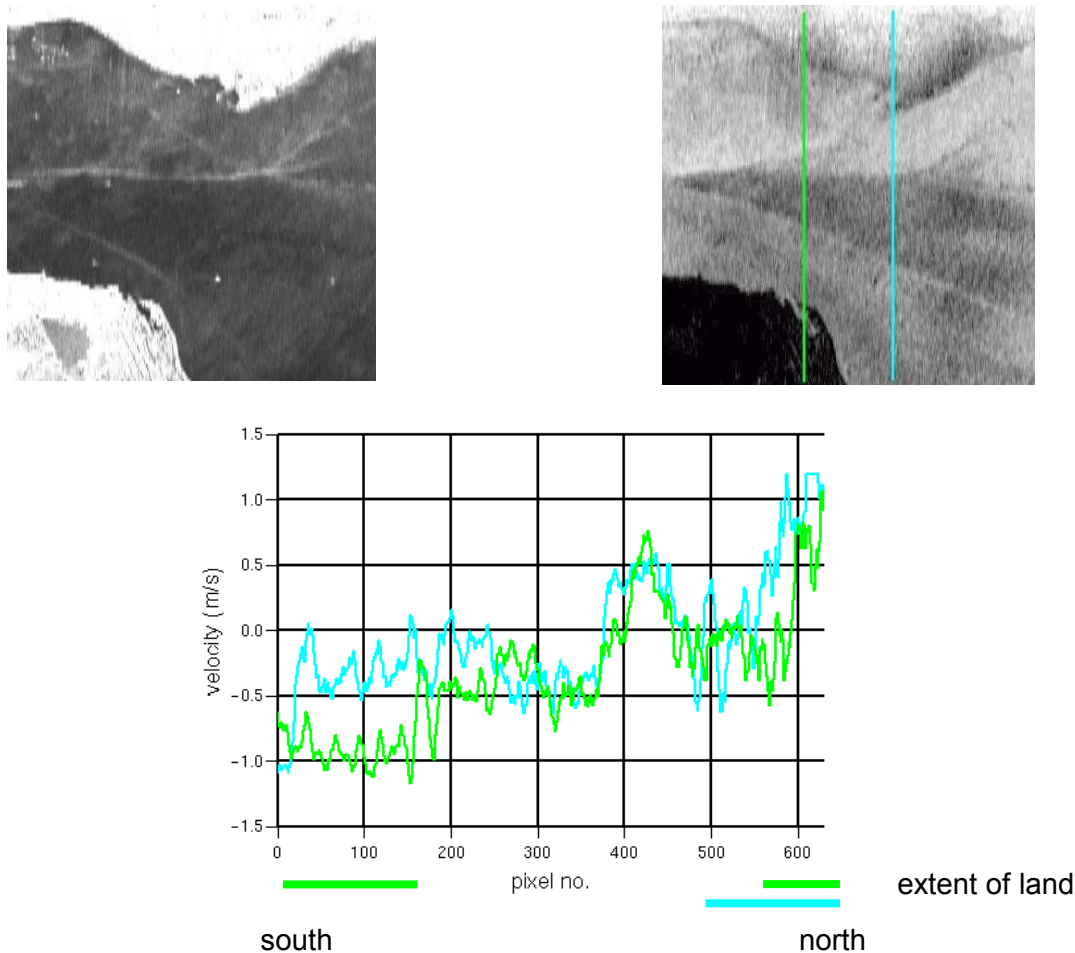


Figure 5: Top left: conventional SAR image of Tay estuary. Top right: image of phase of along-track interferogram, on grey scale from black (-1.6 radians) to white (+1.6 radians). Right: profiles of ground-range component of surface velocity along lines marked in middle figure. The coloured lines under the plot indicate the areas of land on the profile with the corresponding colour.

## COMPARISON WITH OTHER DATA

Both the ADCP and hydrodynamical modelling produced results in terms of x (East-to-West) and y (North-to-South) components. The latter component is in the relevant direction for comparison with the velocities inferred from the ATI results.

### Comparison with Boat Observations: ADCP Data

Direct comparison of ADCP measured velocities with the ATI results is complicated because of the slight differences in tidal height between the data sets and also because every ADCP has a zone where no measurements can be taken. This is known as “the blanking distance”, which is a function of the ADCP’s frequency (see Table 1). However, the effect is negligible in conditions of low surface wind speed, as occurred on the day of the ATI data acquisition. The results from the two available ADCP transects approximately north-to-south from Tayport (Table 4) are presented in Figure 7. The top row of pixels in Figure 7 (top) should be compared with the two profiles in Figure

5 (bottom) from pixels 160 - 500. Both sets of observations show a similar range of velocities (-0.4 to 0.4 m/s for the ADCP data, and -0.5 to +0.6 m/s for the radar data), and they both agree that the higher velocities are on the north side of the Estuary.

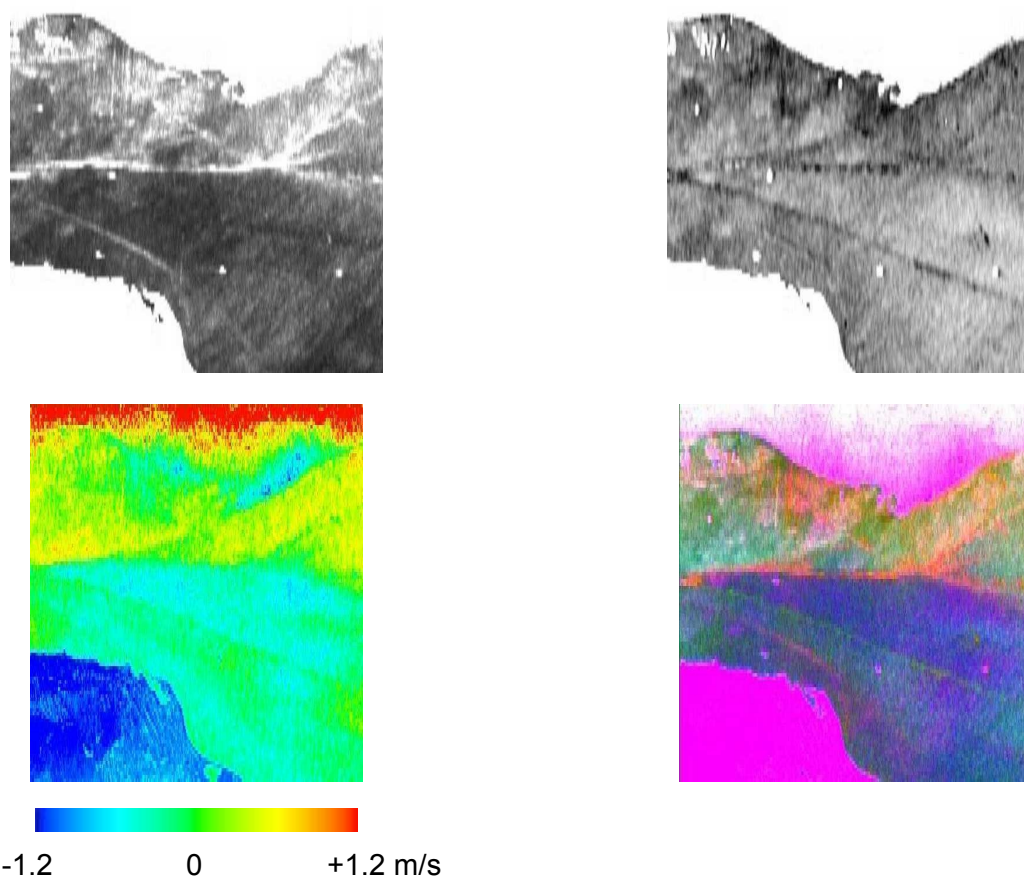


Figure 6: ATI results. Top left: ATI amplitude. Top right: ATI coherence. Bottom left: Range component of surface velocity inferred from ATI phase. Bottom right: Colour composite of ATI amplitude (red), phase (green) and coherence (blue).

Table 4: Time and tidal height of ADCP data acquisitions.

Transect	Tide Height	Time (before high water)
1 (Figure 7, left)	4.3 m	1 hr 03 m to 44 m
2 (Figure 7, right)	4.3 m	34 m to 23 m
3 (data not available)	5.1 m	1 hr 16 m to 52 m
ATI (Figures 5 & 6)	5.2 m	32 m
Numerical model (Figure 8)	5.2 m	29 m

**Surface Flow Measurements from Current Meters and Drift Buoys**

A survey boat with a surface current meter was deployed off Tayport (shown in Figure 1) an hour before the ESAR data acquisition and remained on station for a half hour after data acquisition. Maximum surface flows were observed in the middle of the channel north of Tayport. Velocities ranged from 0.90 to 1.55 m/s on tides of 3.0 to 4.8 m respectively. These are comparable to the values obtained from the ADCPs.

### Comparison with Previous Remote Sensing Research

The location and characteristics of the surface structure of the estuarine fronts identified by the X-band ATI data agree well with the results of the previous remote sensing research (1; Figures 3 and 4 here).

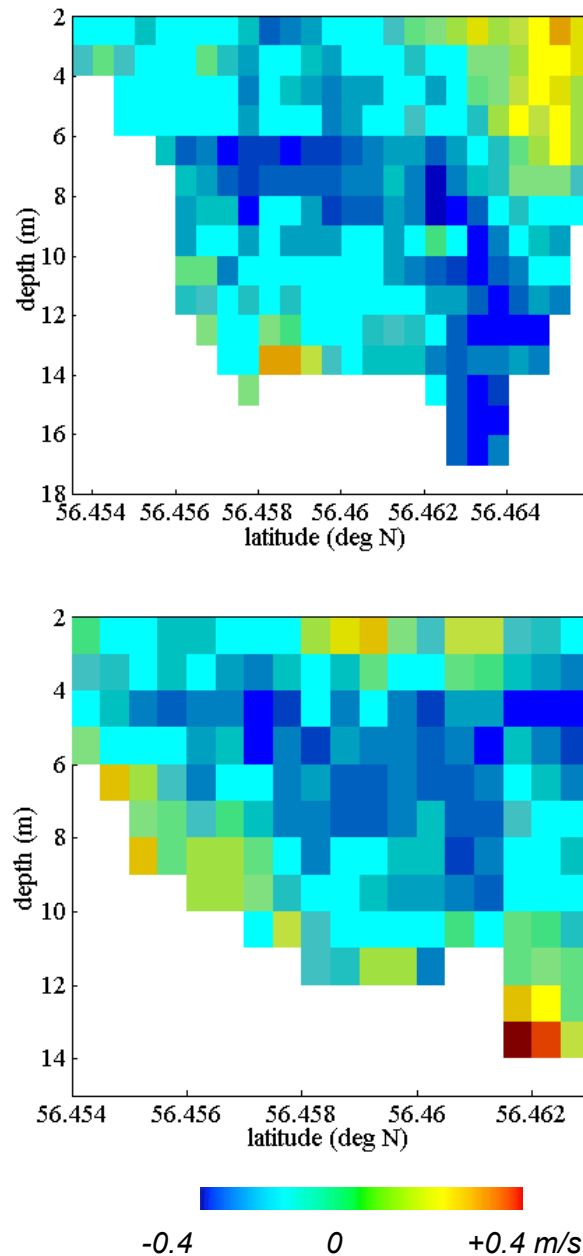


Figure 7: Component of velocity measured in the radar ground-range direction from ADCP observations (top) Transect 1: 1hr 03 min to 44 min before high water (4.3 m tide) and (bottom) Transect 2: 34 to 23 min before high water (4.3 m tide). Transect 1 runs (left to right) from pixels 160 to 500 in the radar data shown in Figure 5.

### Comparison with Hydrodynamic Modelling

Two numerical models, namely the Tidal Flow Development (TFD) and the Tay Estuary Cross-Sectional (TEXSM) (9), were developed for this project. Their characteristics are summarised in Table 5.

Table 5: Characteristics of hydrodynamic models used in this study

Model	Key features	Comments
TFD	2-D, depth-averaged, variable spatial and temporal resolution	Generates flow vectors for whole estuary
TEXSM	2-D, estuarine cross-sectional model	Generates secondary flows associated with buoyant and non-buoyant processes

These models have been used to generate the depth-averaged flow field at the time of the ATI acquisition. To compare the results, the following relationship between surface and depth averaged velocity for the Tay Estuary may be applied :

$$u/u_{mean} = 0.1919 \log_{10}(1-d/d_{max}) + 1.1938 \quad (2)$$

where  $u$  is the velocity at a particular depth;  $u_{mean}$  is depth averaged velocity (i.e. TFD velocity);  $d$  is depth relative to zero at the surface, and  $d_{max}$  is total depth (9).

The modelled surface velocities from the main channel vary from 1.40 to 1.65 m/s, and hence the models predict higher velocities than those measured in situ. Figure 8 shows the modelled component in the radar ground-range direction, where it can be seen that the modelling does not capture all the frontal structure seen in the ATI data in Figures 5 and 6.

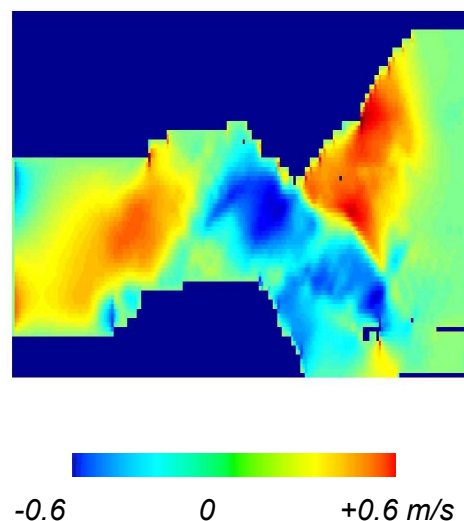


Figure 8: Modelled component of surface velocities in radar range direction, coincident with ATI data acquisition.

## DISCUSSION

A good correlation between the ATI results and the ADCP and surface flow meter measurements has been found. The modelled surface flow velocities, however, are significantly higher than either the ATI or observed measurements. The model predicts a uniform flow up-estuary, whereas the remote-sensing results (Figures 3-6) show that the actual hydrodynamic processes are much more complicated, including two-directional flows, convergent fronts, secondary flows, and many other processes (1). All of these processes will result in significantly higher frictional effects with a consequent reduction in the up-estuary flow velocity. In addition, the hydrodynamic models considered here work most accurately in conditions of reasonably steady flow. Around 30 minutes before high water the velocity gradient changes very rapidly at the Tayport Narrows, introducing a significant source of error into the model. The overall result is that the accuracies of flow velocity and vectors in the TFD model depend on the tidal stage and the location.

The hydrodynamic models used here are accurate to within 10% under reasonably steady flow conditions (around mid-flood and high/low water), increasing to within 25% under conditions of

maximum velocity gradient (from 1 hr to 20 min before high water). This means that observations need to be accurate to within  $\pm 0.15$  m/s to be useable throughout the tidal cycle. The results here imply that the ATI technique can estimate the surface flow velocities to this required accuracy, but further experiments under a range of environmental conditions are needed in order to establish whether this is always the case.

## CONCLUSIONS AND RECOMMENDATIONS

The critical advantage of ATI is its ability to estimate the instantaneous surface flow from a single pass over a whole estuary. This means that it can resolve the complex hydrodynamic processes occurring in estuaries. This is clearly demonstrated in this study where extremely complex hydrodynamic processes occurring over a scale of a few tens of metres have been resolved by the ATI measurements. This unique capability could be applied to a wide range of estuarine modelling applications in the following ways:

- a) Enhancement of two-dimensional models. The ATI results combined with bathymetry and the depth-velocity relationship defined in Equation (2) could be used to initialise and parameterise models.
- b) Optimising future boat-based sampling. Locations and times in the tidal cycle where maximum differences between ATI and modelled flow velocities could be identified and prioritised for additional surveying.
- c) Development of three-dimensional estuarine hydrodynamic models. The location and magnitude of fronts identified from the ATI results, coupled with the flow velocities, could be used as inputs.

This study shows that airborne ATI, with the parameters of the DLR ESAR system, can determine the detailed surface flow patterns that occur in estuaries and can provide a unique, invaluable data source for assisting the management of estuaries. Indeed, more comprehensive information would be obtained from two orthogonal flight directions, which would allow the derivation of vector currents.

## ACKNOWLEDGEMENTS

The ATI data were acquired by DLR as part of the NERC/BNSC SHAC campaign. The ATM and CASI data was acquired by the NERC ATSF facility. We thank the DLR ESAR team, particularly Ralf Horn and Rolf Scheiber, and also Anthony Denniss of Infoterra Ltd. for their assistance during this project. We also thank Scott Couch of Oregon State University for providing the depth-averaged model (TFD) and David Wotherspoon of North of Scotland Water Authority for providing the model bathymetry. The project was supported by EPSRC Grant GR/N37360/01 and NERC Grant DST/26/57. The analysis of the ATI data was initiated under the BNSC NEWTON programme (Contract CU009-017539) and continued under funding from BAE SYSTEMS.

## REFERENCES

- 1 Ferrier G & J M Anderson, 1997. A multi-disciplinary study of frontal systems in the Tay Estuary. Estuarine, Coastal and Shelf Science, 45, 317-336
- 2 Simpson J H & W R Turrell, 1986. Convergent fronts in the circulation of tidal estuaries, Estuarine Variability, Ed. Wolfe (Academic Press).
- 3 Marmorino G O, T F Donato, M A Sletten & C L Trump, 2000. Observations of an inshore front associated with the Chesapeake Bay outflow plume, Continental Shelf Research, 20, 665-684

- 4 Goldstein R M & H A Zebker, 1987. Interferometric radar measurements of ocean surface currents. Nature, 328, 707-709
- 5 Romeiser R & D R Thompson, 2000. Numerical study on the along-track interferometric radar imaging mechanism of oceanic surface currents. IEEE Transactions on Geoscience and Remote Sensing, 38, 446-458
- 6 Schreiber R, 1998. Along- and across-track single-pass interferometry using the E-SAR system. Proc. IGARSS '98 (Singapore) 1097-1099
- 7 Schreiber R et al., 1999. Overview of interferometric data acquisition and processing modes of the experimental airborne SAR system of DLR. Proc. IGARSS 99 (Hamburg) 35-37
- 8 Carande R, 1994. Estimating ocean coherence time using dual-baseline interferometric synthetic aperture radar. IEEE Transactions on Geoscience and Remote Sensing, 32, 846-854
- 9 Neill, S P, 2002. Remote Sensing, In-Situ and Modelling Studies of Tidal Fronts in the Tay Estuary. PhD. Thesis, University of Strathclyde.